

# Analytical Models for Motifs in Temporal Networks: Discovering Trends and Anomalies

Alexandra Porter  
amporter@cs.stanford.edu  
Department of Computer Science  
Stanford University  
Stanford, CA

Baharan Mirzasoleiman  
baharan@cs.ucla.edu  
Department of Computer Science  
University of California Los Angeles  
Los Angeles, CA

Jure Leskovec  
jure@cs.stanford.edu  
Department of Computer Science  
Stanford University  
Stanford, CA

January 3, 2022

## Abstract

Dynamic evolving networks capture temporal relations in domains such as social networks, communication networks, and financial transaction networks. In such networks, temporal motifs, which are repeated sequences of time-stamped edges/transactions, offer valuable information about the networks' evolution and function. However, currently no analytical models for temporal graphs exist and there are no models that would allow for scalable modeling of temporal motif frequencies over time. Here, we develop the *Temporal Activity State Block Model (TASBM)*, to model temporal motifs in temporal graphs. We develop efficient model fitting methods and derive closed-form expressions for the expected motif frequencies and their variances in a given temporal network, thus enabling the discovery of statistically significant temporal motifs. Our TASMB framework can accurately track the changes in the expected motif frequencies over time, and also scales well to networks with tens of millions of edges/transactions as it does not require time-consuming generation of many random temporal networks and then computing motif counts for each one of them. We show that TASBM is able to model changes in temporal activity over time in a network of financial transactions, a phone call, and an email network. Additionally, we show that deviations from the expected motif counts calculated by our analytical framework correspond to anomalies in the financial transactions and phone call networks.

## 1 Introduction

Networks are ubiquitous models for real world systems, with applications ranging from social interactions to protein relationships [14]. Many such systems are not static, but the edges are active only at certain points in time. The networks in which *temporal edges* appear and disappear over time are called time-varying or *temporal networks*. Examples of temporal networks include communication and transaction networks where each link is relatively short or instantaneous, such as phone calls or financial exchanges.

Time dependent and temporal properties can be analyzed on time-varying networks. Extracting recurring and persistent patterns of interaction in temporal networks is of particular interest, as it provides higher order information about the network transformation and functionality [3]. For example, an abundance of triangles in financial transaction networks is associated with anomalies and is identified as the signature of

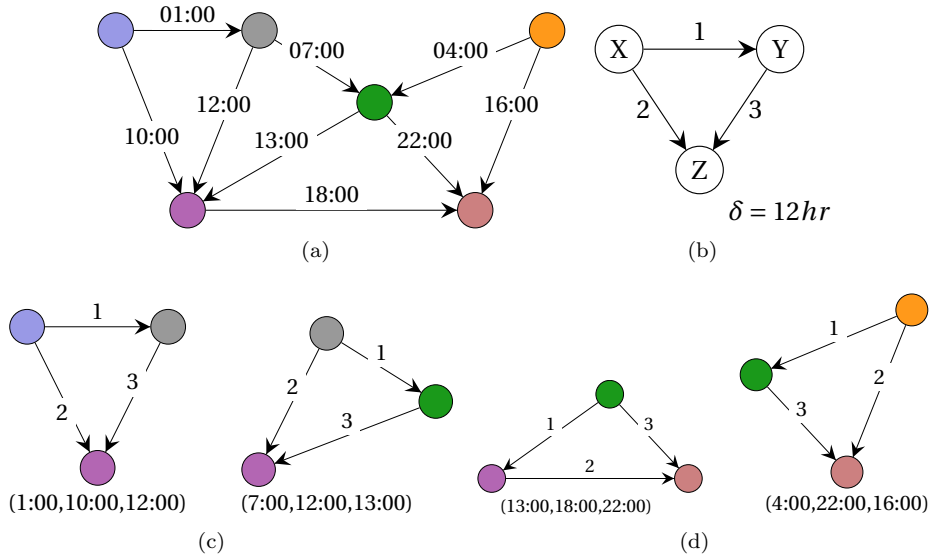


Figure 1: (a) A temporal network with edges appearing over a day, (b) a motif  $M$  with a temporal window of 12 hours, (c) examples of  $M$  in the network, and (d) triangles in the network which are not  $\delta$ -instances of  $M$ , either due to edge order or time between first and last edge.

financial crisis [17]. Similarly, phone calls have been shown to significantly increase in volume and change patterns during major events such as earthquakes [21].

Repeated patterns of interconnections between nodes occurring at a significantly higher frequency than those in randomized networks are called *motifs*. Formally, a *temporal motif* is a subgraph and an ordering on the temporal occurrences of its edges.  $\delta$ -instances of a temporal motif are instances in which all the temporal edges appear according to the ordering specified by the temporal motif within a time window of length  $\delta$  [12, 15]. Figure 1 illustrates a small temporal network with  $\delta$ -instances of a temporal motif  $M$ .

However, currently no statistical models for temporal graphs exist that would allow for modeling frequencies of temporal motifs over time. Modeling of temporal motifs provides two challenges: First, one has to develop a statistical model of a temporal graph, which models temporal dynamics of node activations and who they send their edge/transaction to. And second, even after the model is built, the temporal motif frequencies and their variances need to be established. A naive approach would be to fit the model, generate/materialize a number of synthetic graphs from the model, and then apply expensive temporal motif counting algorithms in order to establish expected motif frequencies and their variances. Obviously such approach is infeasible and computationally too expensive and thus a new approach is needed.

Here we propose the *Temporal Activity State Block Model (TASBM)*, which allows for efficient computation of expected temporal motif frequencies and their variances. TASBM solves both above challenges: we provide an efficient model parameter fitting technique that scales *linearly* with the number of temporal edges in the graph; moreover, we also provide a *constant time* method for computing motif frequencies and their variances. This is in sharp contrast to naive approaches that would require exponential time.

The key to our approach is to develop a model where motif frequencies can be analytically derived and this computed in constant time (where the constant depends on the motif size and number of groups in TASBM, both of which are fixed constants and usually small). TASBM models different activity levels of groups of nodes in a temporal network and can effectively capture intermittent activation between individual nodes. More precisely, our proposed TASBM model first partitions the nodes into different groups based on their activity level, *i.e.*, the rate of temporal edges they are likely to send or receive. We then model rate of out-links and in-links between every pair of groups using Poisson processes. Every pair of groups has distinct rate for sending and receiving temporal edges. The nodes' activity level, and hence their group assignment, may change over time. Furthermore, TASBM allows the rates of the Poisson processes to vary over time, and hence is able to robustly and efficiently model the bursty arrival of temporal edges that is observed in

a real temporal network. Therefore, it allows for accurate identification of temporal network properties.

We conduct experiments on both synthetic and real-world temporal networks. Results on synthetic networks demonstrate that our analytical framework can closely track the changes in the frequencies of  $\delta$ -instances of temporal motifs over time. When applying our framework to analyze synthetic networks containing planted anomalous motifs, our results show that although the planted motif anomalies cannot be identified based on motif counts alone, they can be discovered through comparison to the expected frequencies provided by our analytical model.

In our real-world experiments, we apply our analytical model to a subset of a financial transaction network with 118.7 thousand nodes and 2.9 million temporal edges. In addition, we apply our framework to find trends in a phone call network with 1.2 million nodes and 21.9 million temporal edges, and a subset of an email network with 997 nodes and 307,869 edges. Our method can accurately track motif frequencies in the most significant community of the financial network. In the full financial network, it successfully localizes the anomalies caused by a financial crisis. In the phone call network, we observe that our analytical framework can identify weekly phone call trends such as peak hours and weekends.

## 2 Related Work

In this section, we review the related work to dynamic network and activity state models, as well as temporal motifs.

**Dynamic network models.** There is a body of work on modeling dynamic networks, mostly by extending a static model to the dynamic setting [1, 5, 8, 18–20]. Among the existing methods, temporal extensions of stochastic block models (SBMs) are the most relevant to our work. In particular, a dynamic SBM, in which a transition matrix specifies the probability of nodes to switch classes over time [8, 20]. However, in contrast to our work here the above works both assume that edge probabilities do not change over time. More recently, models in which the network snapshots are modeled using SBM [5, 19], and the state evolution of the dynamic network is modeled by a stochastic dynamic system have been proposed. Other temporal extensions of block model include [4], which presents a non-stationary extension of the SBM; and [13] that performs clustering on temporal networks, and uses Markov chains to model node groups. Our work here differs in that it focuses on temporal graphs, the model allows for linear time fitting and provides closed form expressions for temporal motif counts.

**Temporal motifs.** Paranjape et. al. [15] extended the concept of static motifs to temporal networks and proposed a framework for counting the exact number of relatively small temporal motifs. Very recently, [12] proposed sampling methods for approximating the number of temporal motifs. Existing methods either do not account for ordering of the temporal edges [22], or require temporal edges in a motif to arrive consecutively to a node [10]. Among other examples are the algorithm of [7] that uses ideas from sub-sequence mining to identify patterns in temporal graphs, and methods of [16] for finding temporal isomorphic subgraphs. While this line of work aims to accurately count or approximate the actual numbers of motif instances in any graph, the goal of our work is to determine the expected number and variance of motif instances in a graph, given its underlying statistical model.

Currently no statistical model of motifs in temporal graphs exists. However, there have been several heuristic/empirical techniques proposed. Such approaches are based on generating a large ensemble of randomized temporal networks and include shuffling and reversing of timestamps [2, 6, 9–11]. Unlike these heuristic/empirical methods, we develop a statistical model and closed-form expressions for motif counts and their variances. Crucially, our approach does not require expensive shuffling/simulation of network ensembles, and this scales well to large temporal networks.

## 3 Network Activity Model

In this section we describe our Temporal Activity State Block Model (TASBM). Our goal is to construct a temporal network model which can be updated efficiently and thus maintained online, so that it can be

used to describe the network before the full edge set is known.

Formally, a *temporal graph* can be viewed as a sequence of static directed graphs over the same (static) set  $V$  of  $n = |V|$  nodes and the set  $E$  of  $m = |E|$  *temporal edges*. Each *temporal edge* is a timestamped ordered pair of nodes  $(e_i = (u, v), t_i), i \in [m]$ , where  $u, v \in V$  and  $t_i \in \mathbb{R}$  is the timestamp at which the edge arrives. For example, in a phone call network, each temporal edge includes the caller,  $u$ , the receiver,  $v$ , and the time,  $t_i$  at which the call was placed. Multiple temporal edges between the same pair of nodes  $u$  and  $v$  and different timestamps can exist. We assume that the timestamps  $t_i$  are unique so that the temporal edges may be strictly ordered. However, our methods do not rely on this assumption and can easily be adapted to the case where timestamps are not unique, e.g. by consider each possible ordering of edges with a shared timestamp or selecting an order at random.

The *stochastic block model* [5] on static networks is defined as dividing the nodes into communities, or blocks, such that a higher proportion of the possible edges within a block occur, compared to those between blocks. We propose a temporal variant of the stochastic block model in which we partition the nodes of the network into groups based on their activity levels, which we define as the rates at which in- and out-edges arrive to nodes. This means that a particular block is a set of vertices with *similar temporal activity*. Specifically, nodes within each block will all have similar rates of out- and in- edge arrivals.

### 3.1 Temporal Activity State Block Model

In our Temporal Activity State Block Model (TASBM) we consider two sets of groups or activity states  $G^{in} = \{1, \dots, C^{in}\}, G^{out} = \{1, \dots, C^{out}\}$ . Every node  $u$  in the network belongs to a group  $a_u^{in} = i \in G^{in}$  based on its activity level for receiving in-links and a group  $a_u^{out} = j \in G^{out}$  based on its activity level for sending out-links. Nodes in the same group  $i \in G^{in}$  have similar rate of receiving temporal edges. Similarly, nodes in the same group  $j \in G^{out}$  have similar rate of sending temporal edges. We model group assignments  $a_u^{in}, a_u^{out}$  for  $u \in V$  as independent draws from multinomial distributions parameterized by  $\pi^{in}, \pi^{out}$ . Thus,  $a_u^{in} \sim \text{Multinomial}(\pi^{in})$ , and  $a_u^{out} \sim \text{Multinomial}(\pi^{out})$ .

We consider a  $C^{out} \times C^{in}$  matrix  $\theta$  such that  $\theta_{ij}$  denotes the rate of temporal edges from nodes in group  $i \in G^{out}$  to the nodes in group  $j \in G^{in}$ . After assigning nodes to different activity states, we model the temporal edges between every pair  $(u, v)$  of nodes with  $a_u^{out} = i, a_v^{in} = j$  as independent Poisson draws, where the means of these Poisson draws are specified by  $\theta_{ij}$ . More formally, every temporal edge  $(e_r = (u, v), t_r)$  between the node  $u$  in out-link activity state  $a_u^{out} = i$  to the node  $v$  in in-link activity state  $a_v^{in} = j$  is an independent Poisson draw. I.e.,

$$e_r = (u, v) | a_u^{out} = i, a_v^{in} = j \sim \text{Poisson}(\theta_{ij}).$$

For the ease of notation, instead of  $\theta_{a_u^{out} a_v^{in}}$ , we subsequently use  $\theta_{a_u a_v}$  to denote the rate of out-links from nodes in activity state  $a_u$  to the nodes in activity state  $a_v$ .

As nodes change their activity level over time, we assign individual nodes to a state based on their activity levels on each time window  $T$ . Then we model arrivals of temporal edges between each pair of nodes as a Poisson process with a constant parameter on time intervals of length  $T$ . Note that the rates of the Poisson processes can vary for each time window, and hence TASBM is able to robustly and efficiently model the bursty arrival of temporal edges that is observed in a real temporal network.

### 3.2 Parameter Inference in TASBM

For all pairs of vertices  $(u, v)$  such that  $a_u^{out} = i$  and  $a_v^{in} = j$  for some  $i \in G^{out}$  and  $j \in G^{in}$ , the Poisson process modeling temporal edges between  $u$  and  $v$  will be parameterized by a constant  $\theta_{ij} = \theta_{a_u a_v}$  in every time interval of length  $T$ . Across intervals, we calculate the posterior model parameters  $\alpha$  and  $\theta$  as:

$$\hat{\alpha} = \frac{n_r}{n}, \hat{\theta}_{rs} = \frac{m_{rs}}{n_r n_s},$$

where we denote by  $n_r$  the number of nodes in group  $r$ , and by  $m_{rs}$  the number of edges connecting group  $r$  to group  $s$  in a time interval of length  $T$ . Model inference can be done in at most two passes over the

edges and in practice, can be well-approximated in one pass (see Section 5.1 for details). Thus, this method is extremely scalable and runs in time *linear* in the number of edges in the graph.

## 4 Analytical Model for Temporal Motifs

Having defined the model our next task is to “count” the motifs. In fact, we do not want to count them as counting would mean materializing/sampling many networks from the model and then running expensive motif counting algorithms. Rather, we will analytically derive closed-form expressions that allow us to quickly calculate motif counts and their frequencies.

We first provide formal definitions of temporal motifs and  $\delta$ -instances of temporal motifs. We then introduce our analytical framework for calculating expectation and variance of the number of motif instances. Finally, we provide the computational complexity of our method and show that it can easily scale to large real-world temporal networks with millions of temporal edges.

### 4.1 Temporal Network Motifs

Formally, a temporal motif  $M$  defines a particular sequence of interactions between a set of nodes over time.

**Definition 1** (temporal motif). *A  $k$ -node  $z$ -edge temporal motif  $M = (G_M, \prec_M)$  consists of a graph  $G_M = (V_M, E_M)$ , such that  $|V_M| = k$  and  $|E_M| = z$ , and a strict total ordering  $\prec_M$  on the edges  $E_M$ . We index  $E_M = \{e'_1, \dots, e'_z\}$ , such that  $e'_1 \prec_M e'_2 \prec_M \dots \prec_M e'_z$ .*

Note that multiple interactions between the same pair of nodes may occur in the sequence defined by  $M$ , but each edge is indexed and ordered uniquely. In a dynamic network, any subgraph of a temporal graph is a  $\delta$ -instance of a temporal motif  $M$  if it is isomorphic to  $G_M$ , the set of its temporal edges follows the same ordering imposed by  $M$ , and it occurs within a time window of  $\delta$ .

**Definition 2** ( $\delta$ -Instance of a temporal motif). *A temporal subgraph  $G_s = (V_s, E_s)$ , with  $E_s = \{(e_1, t_1), \dots, (e_z, t_z)\}$  is a  $\delta$ -instance of a temporal motif  $M$  if 1) isomorphism: there exist an edge-preserving bijection  $f : V_s \rightarrow V_M$  between nodes of the subgraph and nodes of the motif such that  $\forall_{e=(u,v) \in E_s} (f(u), f(v)) \in E_M$ ; 2) temporal ordering: the edges of the temporal motif occur according to the ordering  $\prec_M$ , i.e., for the ordered sequence  $f(e_h) \prec_M f(e_i) \prec_M \dots \prec_M f(e_j)$  we get a set of strictly increasing timestamps  $t_h < t_i < \dots < t_j$ ; and 3) temporal window: all the edges in  $E_s$  occur within  $\delta$  time, i.e.  $t_j - t_h \leq \delta$ .*

Here, our goal is to derive the expected number (and the variance) of  $\delta$ -instances of a given temporal motif in a time-varying network. More precisely, given the number of nodes and degree distribution of a temporal network at each point in time, we are interested in calculating the expected frequency of ordered subsets of edges from the temporal network that are  $\delta$ -instances of a particular temporal motif. In the following, we present a general analytic approach, and show how to apply this approach to the Temporal Activity State Block Model (TASBM).

### 4.2 Expected Motif Frequencies for $T \leq \delta$

Next we provide a closed form solution for the expected  $\delta$ -instances of temporal motifs in TASBM networks. To calculate the expected number of  $\delta$ -instances of a temporal motif over a time window of length  $T$ , we need to calculate the expected number of subgraphs  $G_s = (V_s, E_s)$  satisfying the conditions specified in Definition 2. The following Theorem summarizes our main theoretical results.

**Theorem 1.** *The expected number of  $\delta$ -instances of a  $k$ -node  $z$ -edge temporal motif  $M$  in a network with a set  $V$  of nodes modeled by a TASBM with  $C$  states during a time interval  $[t_0, t_0 + T)$  for  $T \leq \delta$  is*

$$\mathbb{E}[N_M | T \leq \delta] = \mathbb{E}[N_{S_{V,C}^{k,z}}] \cdot Pr(t_0 \leq t_1 < t_2 < \dots < t_z < t_0 + T),$$

where the first term is the expected number of  $k$ -node  $z$ -edge isomorphic subgraphs to the motif graph  $G_M$  in a temporal network with  $V$  nodes modeled by a TASBM with  $C$  states; and the second term is the probability that timestamps of the edges in each isomorphic subgraph occur in the order  $\prec_M$  specified by the motif in a time window of length  $\delta$ .

In the rest of this section, we explain in detail how we derive the above quantities and calculate a closed form solution for the expected number of  $\delta$ -instances of a temporal motif.

**Expected Number of Isomorphic Subgraphs.** We start by calculating the number of ways that subgraphs isomorphic to the motif graph  $G_M$  may occur in the temporal network. In a static network, the number of subgraphs isomorphic to  $G_M$  is equal to the number of unique edge-preserving bijections between nodes of the network and nodes of the motif  $M$ . However, in a temporal graph multiple edges may appear between every pair of nodes in a time interval of length  $T$ , and therefore each bijection may result in multiple isomorphic subgraphs to  $G_M$ . To calculate the number of isomorphic subgraphs, we first compute the number of unique bijections  $f : V_s \rightarrow V_M$  between the nodes of every  $k$ -node  $z$ -edge subgraphs  $G_s = (V_s, E_s)$  and  $G_M = (V_M, E_M)$ . Then we compute the number of isomorphic subgraphs that may result from each bijection  $f$  in a time interval of length  $T$ .

In general, in a graph with  $n$  nodes, there are  $\binom{n}{k}$  ways to choose nodes to form a  $k$ -node subgraph. Furthermore, there are  $k!$  permutations of a set of  $k$  nodes, each corresponding to a unique bijection from  $V_M$  to  $V_s$ . For example, the motif in Figure 1b has  $3! = 6$  possible vertex bijections to a 3-node 3-edge graph (see Appendix Figure 9).

Therefore, the number of bijections  $\mathcal{B}_{k,V}$  between nodes of the temporal network and nodes of the motif is

$$|\mathcal{B}_{k,V}| = \binom{n}{k} k! = P(n, k).$$

We now derive the number of ways that subgraphs isomorphic to the motif graph  $G_M$  may occur in the Temporal Activity State Block Model (TASBM). Here, we first calculate the number of ways nodes in different activity states can form a  $k$ -node subgraph. Any node in the subgraph can be selected from at most  $C$  activity states. Hence, the number of activity state assignments  $\mathcal{A}_{C,k}$  for  $k$  nodes in TASBM is<sup>1</sup>

$$|\mathcal{A}_{C,k}| \leq C^k$$

To compute the number of bijections, assume that nodes of the temporal graph are partitioned into  $C$  activity states as  $V = \{V^1, \dots, V^C\}$ , and let  $n^c = |V^c|$  be the number of nodes in activity state  $c \in [C]$ . Consider an activity state assignment  $A = \{a_1, \dots, a_k\} \in \mathcal{A}_{C,k}$ , where  $a_i \in [C]$  is the activity state of the  $i$ -th node. We now calculate the number of subsets  $V_s$  of  $k$  nodes in the network that are consistent with the activity state assignment  $A$  (see Appendix Figure 11 for an example of activity states mapped to nodes). Let  $n_A^c$  be the number of nodes in  $A$  that are assigned to the activity state  $c$ . There are  $\binom{n^c}{n_A^c}$  ways to select  $n_A^c$  nodes from  $V^c$ . Therefore, there are  $\binom{n^1}{n_A^1} \dots \binom{n^C}{n_A^C}$  ways of forming a  $k$ -node subgraph in the network that are consistent with the activity state assignment  $A$ . Finally, for each permutation of the  $n_A^c$  nodes in activity state  $c$  we get a bijection. Hence, the number of unique bijections in TASBM is

$$|\mathcal{B}_{k,V,C}| = \sum_{A \in \mathcal{A}_{C,k}} \prod_{c \in [C]} P(n^c, n_A^c), \quad (1)$$

where  $P(n^c, n_A^c) = \binom{n^c}{n_A^c} n_A^c!$  is the number of  $n_A^c$ -permutations of  $n^c$ . Note that  $\prod_{c \in [C]} P(n^c, n_A^c)$  is constant for every activity state assignment  $A \in \mathcal{A}_{C,k}$ , and hence the cost of calculating Eq. 1 only depends on the number of possible activity state assignments  $O(C^k)$ .

<sup>1</sup>If some groups have fewer than  $k$  nodes, we have  $|\mathcal{A}_{C,k}| < C^k$ . For example, let  $k = 3$  and  $s_i$  be the number groups of size  $i$  for  $i \in \{0, 1, 2\}$ , then  $|\mathcal{A}_{C,k}| = (C - s_0)^k - s_1 \binom{k}{2} (C - 1 - s_0) - s_2$ . If each node is in a separate group with  $C = |V|$  we get  $|\mathcal{B}_{k,V,n}| = |\mathcal{B}_{k,V}| = P(n, k)$ .

Next, we calculate the expected number of isomorphic subgraphs that can result from each bijection in a time interval of length  $T$ . As we discussed in Section 4.1, in the TASBM the arrival rate of temporal edges between any pair of nodes  $(u, v)$  depends on their activity states. The expected number of temporal edges that occur from node  $u$  in activity state  $a_u$  to node  $v$  in activity state  $a_v$  in an interval  $[t_0, t_0 + T]$  is

$$\mathbb{E}[N_{e_{uv}} | t \in [t_0, t_0 + T]] = \int_{t_0}^{t_0+T} \theta_{a_u a_v}(t) dt,$$

where  $\theta_{a_u a_v}(t)$  is the temporal edge arrival rate from activity state  $a_u$  to activity  $a_v$  at time  $t$ .

Let  $f : V_s \rightarrow V_M$  be a bijection, where  $V_s$  is a  $k$ -node subgraph that is consistent with the activity state assignment  $A \in \mathcal{A}_{C,k}$ . In other words,  $V_s = \{v_1, \dots, v_k | a_{v_i} = A[i]\}$ . We now calculate the expected number of  $k$ -node  $z$ -edge isomorphic subgraphs  $S_{V,C,f}^{k,z}$  that can result from  $f$  in a TASBM with nodes  $V$  partitioned into  $C$  activity states, in a time interval of  $[t_0, t_0 + T]$ .

$$\mathbb{E}[N_{S_{V,C,f}^{k,z}} | t \in [t_0, t_0 + T]] = \prod_{\substack{u,v \in V_s, \\ (f(u), f(v)) \in E_M}} \int_{t_0}^{t_0+T} \theta_{a_u a_v}(t) dt. \quad (2)$$

Note that for each activity state assignment  $A \in \mathcal{A}_{C,k}$ , the expected number of subgraphs for all the  $\prod_{c \in [C]} P(n^c, n_s^c)$  bijections corresponding to  $A$  is the same. Therefore, from Eq. 1 and 2 we get the following lemma.

**Lemma 1.** *The expected number of  $k$ -node subgraphs isomorphic to the motif subgraph  $G_M$  in a Temporal Activity State Block Model (TASBM) during a time interval  $[t_0, t_0 + T]$  for  $T \leq \delta$  is*

$$\begin{aligned} \mathbb{E}[N_{S_{V,C}^{k,z}} | t \in [t_0, t_0 + \delta]] = \\ \sum_{A \in \mathcal{A}_{C,k}} \prod_{c \in [C]} P(n^c, n_s^c) \prod_{\substack{u,v \in V_s | R(V_s) = A, \\ (f(u), f(v)) \in E_M}} \int_{t_0}^{t_0+T} \theta_{a_u a_v}(t) dt, \end{aligned}$$

where  $R(V_s) = A$  is the set of all  $k$ -node subgraphs consistent with activity state assignment  $A$ .

**Probability of Temporal Ordering for  $T \leq \delta$ .** We now compute the probability that the second and third conditions in Definition 2 are satisfied. Precisely, we calculate the probability that for an isomorphic subgraph  $G_s = (V_s, E_s)$ , the timestamps of the mapped edges ordered by  $\prec_M$  are strictly increasing and within a time window of  $\delta$ .

For ease of notation, we subsequently assume that for each subgraph  $G_S$  and corresponding bijection  $f : V_s \rightarrow V_M$ , we have  $f(e_1) \prec_M f(e_2) \prec_M \dots \prec_M f(e_z)$ . Therefore, we need to calculate the probability that  $t_0 \leq t_1 < t_2 < \dots < t_z < t_0 + \delta$ .

The marginal probability for a temporal edge  $e = (u, v)$  from activity state  $a_u$  to activity state  $a_v$  to occur at time  $t$  in the time window  $[t_0, t_0 + T]$  is

$$\Theta_{e=(u,v)}^{[t_0, t_0+T]}(t) = \frac{\theta_{a_u a_v}(t)}{\int_{t_0}^{t_0+T} \theta_{a_u a_v}(t') dt'}.$$

**Lemma 2.** *The probability that temporal edges of a subgraph  $G(V_s, E_s)$  occur in the order  $\prec_M$  specified by motif  $M$  in an interval  $[t_0, t_0 + T]$  is*

$$\begin{aligned} Pr(t_0 \leq t_1 < t_2 < \dots < t_z < t_0 + T) = \\ \int_{t_0}^{t_0+T} \Theta_{e_1}^{[t_0, t_0+T]}(t_1) \int_{t_1}^{t_0+T} \Theta_{e_2}^{[t_0, t_0+T]}(t_2) \dots \\ \int_{t_{z-1}}^{t_0+T} \Theta_{e_z}^{[t_0, t_0+T]}(t_z) dt_z dt_{z-1} dt_{z-2} \dots dt_1. \end{aligned}$$

Note that in the above equation, if the edge arrival rates  $\theta_{ij}$  between activity states do not change in interval  $[t_0, t_0+T)$ , the marginal probability for every temporal edge to happen is  $1/T$ . Hence, every ordering of the temporal edges in the subgraph has a probability of  $1/z!$ . Therefore, for constant edge arrival rates we have  $Pr(t_0 \leq t_1 < t_2 < \dots < t_z < t_0+T) = 1/z!$ . On the other hand, varying edge arrival rates in  $[t_0, t_0+T)$  can be modeled by integrable functions, for which we can calculate the value of the nested integrals to get the probability of the correct ordering  $Pr(t_0 \leq t_1 < t_2 < \dots < t_z < t_0+T)$ .

Finally, the expected number of  $\delta$ -instances of a motif  $M$  is the number of subgraphs that satisfy all the conditions specified in Definition 2. It can be calculated by multiplying the number of possible isomorphic subgraphs to the motif graph  $G_M$  by the probability that timestamps of the edges in each isomorphic subgraph occur in the order  $\prec_M$  specified by  $M$  within a time window of length  $\delta$ .

From Lemma 1 and Lemma 2 we get Theorem 1 for the expected number of  $\delta$ -instances of temporal motifs in a time interval of length  $T \leq \delta$ . The pseudocode of our method is given in Alg. 1.

### 4.3 Expected Motif Frequencies for $T > \delta$

Previously, we calculated the probability of the temporal ordering specified by  $M$  for the case where  $T \leq \delta$ . Next, we consider the scenario where  $T > \delta$ .

Here, the  $\delta$ -instances of a temporal motif may have at least one edge occurring in  $[t_0, t_0+T-\delta)$  or they may have all edges occurring in  $[t_0+T-\delta, t_0+T)$ . Hence, to calculate the expected number of instances in  $T$ , we take a sum over the instances with at least one edge in  $[t_0, t_0+T-\delta)$  and instances fully appearing in  $[t_0+T-\delta, t_0+T)$ .

Similar to the previous section, we need to 1) compute the number of possible isomorphic subgraphs to the motif graph  $G_M$ ; and 2) calculate the probability that timestamps of the edges in each isomorphic subgraph occur in the order  $\prec_M$  specified by the motif within a time window of length  $\delta$ .

In the sequel, we explain the detailed steps in deriving the following Theorem.

**Theorem 2.** *The expected number of  $\delta$ -instances of a temporal motif  $M$  in a Temporal Activity State Block Model (TASBM) during a time interval  $[t_0, t_0+T)$  for  $T > \delta$  is*

$$\mathbb{E}[N_M|T > \delta] = \mathbb{E}[N_M|T = \delta] + \mathbb{E}[N_M|T > \delta, t_1 < t_0 + T - \delta],$$

where  $t_0$  and  $t_1$  are the timestamps of the first and second edges of the motif instance.

**Expected Number of Isomorphic Subgraphs.** To calculate the number of motif instances with the first edge occurring in  $[t_0, t_0+T-\delta)$ , assume that  $e'_1 = (u', v') \in E_M$  is the edge of the motif that comes first in the ordering  $\prec_M$ . We first compute the number of isomorphic 2-nodes subgraphs in the network to  $\{u', v'\}$ . Then, for each isomorphic subgraph, we calculate the number of subgraphs in the remaining network isomorphic to  $V_M \setminus \{u', v'\}$ .

**Lemma 3.** *The expected number of  $k$ -node subgraphs isomorphic to the motif subgraph  $G_M$  in a Temporal Activity State Block Model (TASBM) with the first edge occurring in  $[t_0, t_0+T-\delta)$  for  $T > \delta$  is*

$$\begin{aligned} \mathbb{E}[N_{S_{V,C}^{k,z}} | t_1 \in [t_0, t_0+T-\delta)] = \\ \mathbb{E}[N_{S_{V,C}^{2,1}} | t \in [t_0, t_0+T-\delta)] \cdot \mathbb{E}[N_{S_{V \setminus V_{e_1}, C}^{k-2, z-1}} | t \in [t_1, t_1+\delta)], \end{aligned}$$

where  $t_1$  is the time of appearance of the first edge, and  $V_{e_1}$  is the set of two nodes in subgraph  $S_{V,C}^{2,1}$ .

**Probability of Temporal Ordering for  $T > \delta$ .** We now use marginal edge probabilities to calculate expected frequency on intervals with  $T > \delta$ . For subgraph  $G_S$  isomorphic to  $G_M$ , we compute the probability that the first edge occurs in  $[t_0, t_0+T-\delta]$  and the remaining  $z-1$  edges occur sequentially within a time window of length  $\delta$  starting at  $t_1$ .



---

**Algorithm 1** Calculate Expected Motif Frequency
 

---

**Require:** Set of nodes  $V$ , set of  $C$  activity states, edge arrival rates between activity states  $\theta_{ij}$ , time interval  $[t_0, t_0 + T)$ .

**Ensure:** Expected number of  $\delta$ -instances of motif  $M$  within time interval  $[t_0, t_0 + T)$ .

```

1: for  $(i, j) \in ([C^{out}] \times [C^{in}])$  do
2:    $E[N_{e_{ij}}] = \text{INTEGRATE}(\theta_{ij}, t_0, t_0 + T)$ 
3:  $\mathbb{E}[N_M] = 0$ 
4:  $\mathcal{A}_{C,k}$  = set of  $O(C^k)$  activity state assignments to  $k$  nodes.
5: for  $A \in \mathcal{A}_{C,k}$  do
6:    $|\mathcal{B}_{k,V,C}| = \prod_{c \in [C]} P(n^c, n_s^c)$  ▷ Eq. 1
7:    $V_s = \{v_1, \dots, v_k | a_{v_i} = A[i]\}$ 
8:    $f$  : a bijection from  $V_s$  to  $V_M$ 
9:    $\mathbb{E}[N_S] = 1$ 
10:  for  $(u, v) \in V_s$  such that  $(f(u), f(v)) \in E_M$  do ▷ Eq. 2
11:     $\mathbb{E}[N_S] = \mathbb{E}[N_S] \times E[N_{e_{a_u a_v}}]$ 
12:   $P_{\text{order}} = \text{Pr}(t_0 \leq t_1 < t_2 < \dots < t_z < t_0 + T)$  ▷ Lemma 2
13:   $\mathbb{E}[N_M] = \mathbb{E}[N_M] + |\mathcal{B}_{k,V,C}| \times \mathbb{E}[N_S] \times P_{\text{order}}$ 
return  $\mathbb{E}[N_M]$ 

```

---

**Lemma 4.** *The probability that temporal edges of a subgraph  $G(V_s, E_s)$  occur in the order  $\prec_M$  specified by motif  $M$  in an interval of length  $T > \delta$  with the first edge appearing in  $[t_0, t_0 + T - \delta)$  is*

$$\begin{aligned}
& \text{Pr}(t_2 < t_3 < \dots < t_z < t_1 + \delta | t_1 < t_2, t_1 \in [t_0, t_0 + T - \delta)) = \\
& \int_{t_0}^{t_0 + T - \delta} \Theta_{e_1}^{[t_0, t_0 + T - \delta]}(t_1) \int_{t_1}^{t_1 + \delta} \Theta_{e_2}^{[t_1, t_1 + \delta]}(t) \int_{t_2}^{t_1 + \delta} \Theta_{e_3}^{[t_1, t_1 + \delta]}(t_3) \\
& \dots \int_{t_{z-1}}^{t_1 + \delta} \Theta_{e_z}^{[t_1, t_1 + \delta]}(t_z) dt_z dt_{z-1} dt_{z-2} \dots dt dt_1.
\end{aligned}$$

The expected frequency of  $\delta$ -instances of temporal motif  $M$  in a time window of length  $T > \delta$ , conditional on at least one edge occurring in  $[t_0, t_0 + T - \delta)$ , can be calculated using Lemmas 3 and 4.

$$\begin{aligned}
\mathbb{E}[N_M | T > \delta, t_1 < t_0 + T - \delta] &= \mathbb{E}[N_{S_{V,C}^{k,z}} | t_1 \in [t_0, t_0 + T - \delta)]. \tag{3} \\
& \text{Pr}(t_2 < t_3 < \dots < t_z < t_1 + \delta | t_1 < t_2, t_1 \in [t_0, t_0 + T - \delta))
\end{aligned}$$

Finally, The expected number of instances fully appearing in  $[t_0 + T - \delta, t_0 + T)$  can be calculated from Theorem 1. Hence, we get Theorem 2 for the expected number of  $\delta$ -instances of temporal motif  $M$  in a time interval  $T > \delta$ .

#### 4.4 Variance of motif counts

We next discuss how we can use our framework for deriving the variance of the number of motif instances  $\mathbb{V}[N_M]$ . I.e.,

$$\mathbb{V}[N_M] = \mathbb{E}[N_M^2] - \mathbb{E}[N_M]^2.$$

While we can simply calculate  $\mathbb{E}[N_M]^2$  using Algorithm 1, computing  $\mathbb{E}[N_M^2]$  involves calculating the expected number of *pairs* of  $\delta$ -instances of motif  $M$ . A pair of instances can overlap in up to  $k$  vertices and up to  $z$  temporal edges.

In order to calculate  $\mathbb{E}[N_M^2]$ , we need to consider both independent and dependent pairs of  $\delta$ -instances of  $M$ . Motifs instances which do not share an edge (see Appendix Figures 10a and 10b for examples) are

conditionally independent. On the other hand, pairs of instances which share at least one edge are not independent. For dependent instances, we must consider all possible total orderings of the edges of the two pairs of  $\delta$ -instances of  $M$ . For example there is a pair of  $\delta$ -instances such that  $t_1 < t_2 < t_3 = t_{3'}$  from the first  $\delta$ -instance and  $t_{1'} < t_{2'} < t_{3'} = t_3$  from the second  $\delta$ -instance, but the ordering of the edges  $\{t_1, t_2, t_{1'}, t_{2'}\}$  is not fully specified by the two instances and thus we need to calculate all the possibilities for the remaining 4 edges, including  $t_1 < t_2 < t_{1'} < t_{2'}$ ,  $t_1 < t_{1'} < t_2 < t_{2'}$ ,  $t_{1'} < t_{2'} < t_1 < t_2$ , etc (see Appendix Figure 10c).

Let  $S_1, S_2$  be a pair of  $\delta$ -instances of  $M$ . The time interval that the edges  $E_{S_1} \cup E_{S_2}$  of both instances may occur is within an interval  $[t_0 + \delta, t_0 + 2\delta)$ , depending on which temporal edges, if any, are shared. We denote by  $\mathbb{E}_\delta$  and  $\mathbb{E}_{\delta'}$  expected  $\delta$ - and  $\delta'$ -instances of motif  $M$ , respectively. Then by linearity of expectation, we get

$$\mathbb{E}[N_M^2] = \sum_{\substack{(S_1, S_2): \\ E_{S_1} \cap E_{S_2} = \emptyset}} \mathbb{E}_\delta[N_{S_1} | t \in [t_0, t_0 + T)] \mathbb{E}_\delta[N_{S_2} | t \in [t_0, t_0 + T)] + \sum_{\substack{(S_1, S_2): \\ E_{S_1} \cap E_{S_2} \neq \emptyset}} \sum_{\delta' \in [t_0 + \delta, t_0 + 2\delta)} \mathbb{E}_{\delta'}[N_{S_1 \cup S_2} | t \in [t_0, t_0 + T)].$$

## 4.5 Computational Complexity

Here, we derive the computational complexity of our method to compute the expected number of  $\delta$ -instances of a  $k$ -node  $z$ -edge temporal motif in a TASBM with  $C$  activity states. The first for loop (line 2) in Alg. 1 calculates  $C^2$  integrals to get the expected number of edges between every pair of activity states. For each of the  $|\mathcal{A}_{C,k}| = O(C^k)$  activity state assignments (line 5), we iterate over  $z$  edges (line 10) to calculate the expected number of isomorphic subgraphs. Then we calculate the probability of the correct temporal ordering for the edges of the isomorphic subgraphs (line 12). If edge arrival rates between activity states do not change within the time interval, the probability of correct ordering is a constant ( $1/z!$ ). In the general case, this involves calculating a set of  $z$  integrals as specified in Lemma 2. Assuming the cost of computing each integral is  $O(1)$ , the total computational complexity of Algorithm 1 is  $O(C^k)$ . For the case where  $t > \delta$ , the additional computation of  $\mathbb{E}[N_M | T > \delta, t_1 < t_0 + T - \delta]$  for  $T > \delta$  (Eq. 3) follows the same structure as in the case where  $T \leq \delta$  with different integral bounds. Therefore, the computational complexity for calculating the expected motif frequencies is  $O(C^k)$ , where  $C$  is the number of blocks (usually  $< 10$ ) and  $k$  is motif size (usually  $< 10$ ).

Notice the number of blocks  $C$  and the motif size  $k$  are constant relative to the size of the network, we get a computational complexity of motif counting to be  $O(1)$ . Due to its low computational complexity, our analytical method can easily scale to large real-world temporal networks with millions of temporal edges.

## 5 Experiments

In this section, we present the results of applying our analytical framework to an inferred TASBM to calculate the expected motif frequencies in synthetic and real-world temporal graphs. We compare the expected number of motif instances to the number of observed motif instances counted by the method of [15]. To demonstrate our TASBM model and analytical method, we focus on expected counts for motifs with 2 or 3 nodes and 3 edges (Figure 2).

We first discuss how we fit the TASBM model to observed temporal network data. We then present experiments which show the effect of network properties and model parameters, i.e., average degree of the temporal network, length of the time window  $T$ , and motif window  $\delta$  on how well our model estimates motif frequencies in synthetic data. Next, we show that our analytical framework can accurately track motif frequencies in real-world networks, including a financial transaction network, an email network, and a phone call network. Finally, we show how our model can be used for anomaly detection, by identifying places where the observed counts deviate significantly from the model.

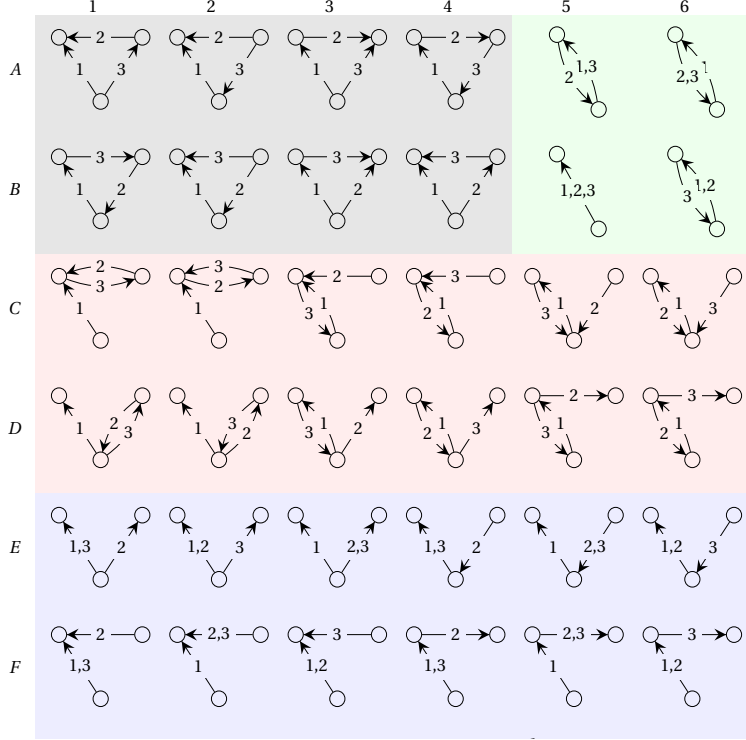


Figure 2: All 2- and 3- node motifs with 3 edges, shaded by main structural feature: triangles (A1-4, B1-4; grey), Two-Node (A5,6 B5,6; green), Reciprocated edge (C1-6,D1-6; red), and Double edge (E1-6,F1-6; blue).

## 5.1 Fitting the TASBM Model

Our framework first computes the average out-edge and in-edge arrival rates for all nodes on every window of  $T$  time units  $[iT, (i+1)T)$ ,  $i \geq 0$ . Out-edge rates are partitioned into  $C^{out}$  groups and in-edge rates are partitioned into  $C^{in}$  groups, for a total of  $C = C^{in} \cdot C^{out}$  groups corresponding to the out- and in-edge rate combinations. In a single pass over the edges of time interval  $[0, T]$ , we can determine the out- and in-degree of each node. To assign our group partitions in a single pass over the nodes at the end of the time interval, we take the following approach. We start by partitioning the full range of possible edge arrival rates, and assign each range to a group. Initially, there are many such groups, i.e. a large value of  $C^{in}$  and  $C^{out}$ . Then nodes are assigned to the group which corresponds to the range containing their observed rate, for out- and in-rates independently. Empty groups can be dropped from subsequent computations, so starting with a large initial set does not incur significant computational cost.

We then use our group assignments to approximate  $\theta$  without making another pass over the edges. During assignment of nodes to groups, we compute the observed average out- and in- degrees of each group in  $[C^{out}]$  and  $[C^{in}]$ , respectively. These total out and in rates correspond to the column and row sums of  $\theta$ . Rather than iterating over all edges once group assignments have been made to determine the exact breakdown of each sum, we make the assumption that the out-edges of a group  $i \in [C^{out}]$  will be distributed among all nodes according to their in-edge rate. Thus we need only the set of average in-rates for each group in  $[C^{in}]$  to determine how the total rate for  $i \in [C^{out}]$  is divided up over a row of  $\theta$ . In practice, this method results in an accurate approximation of  $\theta$ , so we use it for all the following experiments.

## 5.2 Accuracy on Synthetic Networks

Our synthetic networks are generated according to the TASBM with  $C = C^{out} \cdot C^{in}$  groups with  $C^{out}$  out-edge and  $C^{in}$  in-edge states, respectively. Each node is assigned to a group in  $[C]$  chosen uniformly at random.

C	Triangles	Two Vertex	Reciprocated	Double Edge
1	0.229	0.381	0.147	0.381
4	1.99e-05	4.35e-05	2.84e-05	1.69e-05
9	1.89e-05	4.26e-05	2.78e-05	1.60e-05
16	1.04e-05	3.59e-05	2.25e-05	7.90e-06
25	1.04e-05	3.59e-05	2.25e-05	7.91e-06

Table 1: MSRE for varying number of groups  $C$  used by TASBM using  $T=10K$ ,  $\delta=5K$ . The values are calculated over 30 networks generated with 300 nodes and  $C^{out}=C^{in}=5$ .

Each pair of groups  $(C_1, C_2)$  is also assigned an arrival rate, specifying the arrival rate of edges  $(u, v)$  such that  $u \in C_1$  and  $v \in C_2$ . For each pair of nodes  $(u, v)$ , temporal edges are then sampled according to a Poisson process with the rate corresponding to the out-edge group of  $u$  and in-edge group of  $v$ .

**Accuracy of Model Inference.** We first show that we can accurately infer the TASBM parameters used to generate the synthetic network and thus accurately use our analytical approach to determine expected motifs. We measure accuracy of our model over a set of  $r$  synthetic networks, using Mean Squared Relative Error,

$$MSRE = \frac{1}{r} \sum_{i=1}^r \left( \frac{N_M^i - N_M}{N_M^i} \right)^2,$$

where  $N_M^i$  is the actual number of motif instances counted using the method of [15] in the  $i$ -th generated network, and  $N_M$  is the expected motif frequency calculated by our framework.

Table 1 shows MSRE for 30 networks with 300 nodes generated using TASBM with  $C^{out}=C^{in}$ . For generating out-edges, we partition the nodes to groups of size 10, 30, 60, 80, and 120, with out-rates of 1e-7, 1e-6, 1e-5, 1e-4, and 1e-3. For generating in-edges, we have all the nodes in one group, hence having in-rate of 11111e-3. Generated networks have an average of 384,580 edges. We varied the number of groups in our framework for calculating the expected motif frequencies from  $C^{out}=C^{in}=1$  to  $C^{out}=C^{in}=5$  and used  $T=10K$  and  $\delta=5K$  time units. It can be seen that the error quickly vanishes when the model is allowed to use a higher number of groups. However, the improvements from increasing the number of groups quickly diminish. It can be observed that using only  $C^{out}=C^{in}=2$  groups to calculate the expected frequencies, we get almost the same accuracy as using  $C^{out}=C^{in}=5$  groups. This indicates that while real data is likely to have a large variety of node activity levels, a relatively small value of  $C$  can be used to calculate accurate expected motif counts.

**Robustness of Model to Hyper-Parameter Choices.** Next we investigate robustness of our method to choices of hyper-parameters. Figure 3 compares MSRE for 30 networks with 100 nodes generated using TASBM with  $C^{out}=C^{in}=3$ . Here, for generating out-links we divide the nodes into groups of sizes 10, 30, and 60 and use the initial out-rates of 5e-6, 1e-4, and 1e-3, respectively. The rates were chosen to be sufficiently distinct and to generate sufficiently large edge volumes without motif counts exceeding the maximum capacity of the motif counter from [15].

Figure 3a shows the accuracy of our model for networks with increasing average degree, generated by scaling the entire set of arrival rates exponentially, both within and between groups. The peaks in error as the average degree increases occur at approximately the point when motif counts become non-zero, but have high variance due to low edge rates. For two-node motifs, this peak happens at a larger edge volume since the frequency of such motifs are lower than that of three-node motifs.

Figure 3b shows how MSRE converges to zero as the motif window  $\delta$  increases. The convergence is due to the same reason as above; as the motif window increases there is a greater volume of randomly generated edges over which each computation is made, and thus the average motif counts are closer to our expected counts. Again, as there is a smaller number of two-node motifs in a temporal network generated by stochastic block model, the MSRE converges more slowly for two-node motifs.

Figure 3c shows a similar behavior for increasing the length of the time window  $T$ , for a fixed motif window of  $\delta=5K$ .

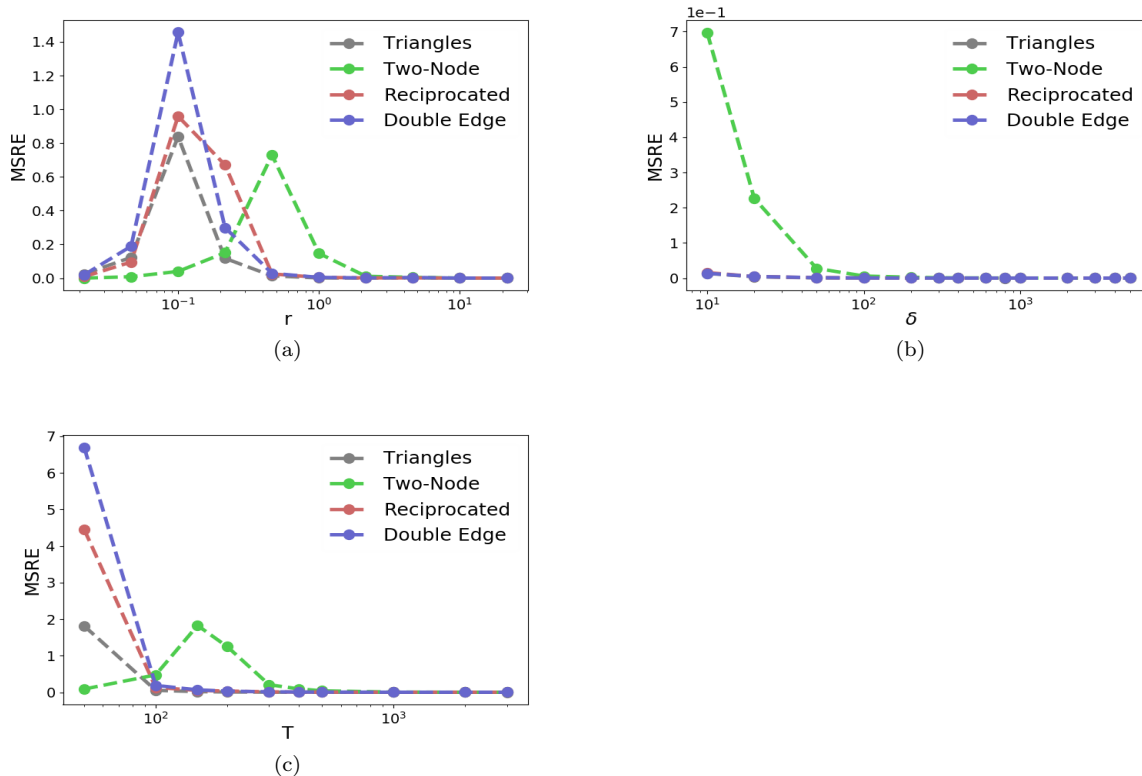


Figure 3: MSRE for the expected motif counts over 30 synthetic networks with 100 nodes for varying (a) number of edges, (b) motif window  $\delta$ , and (c) time window  $T$ . See Figure 2 for motif names. Notice that the TASBM accurately predicts motif counts.

### 5.3 Accuracy on Real-world Networks

In our real-world experiments, we apply our analytical model to a financial transaction network and an email network. We show that our model matches the trends in motif counts in the real data. Since we are interested in modeling temporal dynamics of the networks, we preprocess the financial transaction and email networks by removing low-degree ( $< 10\%$  the largest degree) nodes and focusing on the largest connected community. Due to space constraints we present results for a subset of motifs. Full results can be found in the Appendix.

**Financial Transaction Network.** In our first real-world experiment, we applied our framework to model the motif counts in a small European country’s financial transaction network. The data is collected from the entire country’s transaction log for all transactions larger than 50K Euros over 10 years from 2008 to 2018, and includes 118,739 nodes and 2,982,049 temporal edges. As edges do not occur on weekends, we do not count them toward values of  $T$  and  $\delta$  or in computing edge rates. Figure 4 compares the ground-truth motif counts and the values computed by our model with  $\delta = T = 90$  weekdays for motifs F1 and A6. Notice that TASBM is able to accurately track the changes in motif counts over time.

**Email Network.** We next applied our model to a network of emails exchanged within a European research institution. We use the set of 307,869 temporal edges over 977 nodes, which appear in the 500 days beginning in October of 2003. We modeled and counted frequencies of 2- and 3- node motifs with 3 edges at a time scale of  $\delta = T = 50$  days with 10 intervals. As shown in Figure 5 our model follows the trends in motif counts on the entire network.

**Phone Call Network.** Our final dataset is a temporal network of phone calls made in April 2006 within a

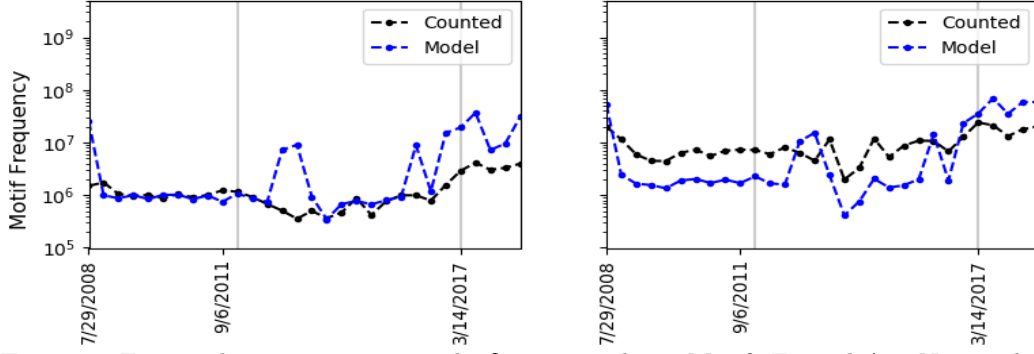


Figure 4: Financial transaction network,  $\delta = T = 90$  days. Motifs F1 and A6. Notice the model accurately tracks the change in motif frequency over time.

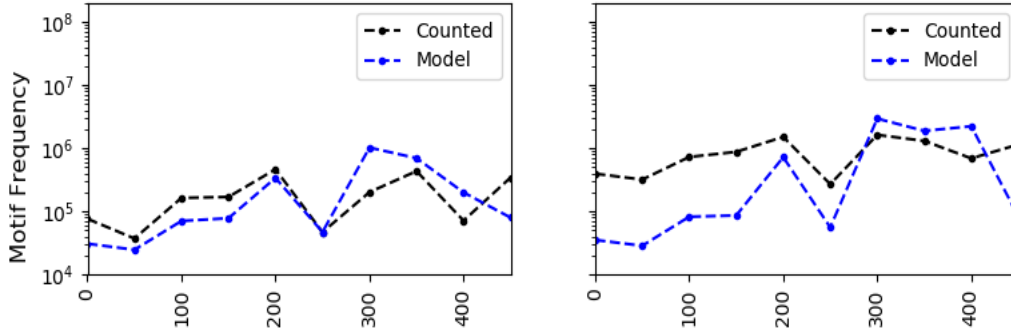


Figure 5: Email network,  $\delta = T = 50$  days. Motifs F1 and A6. Notice the model accurately tracks motif counts over time.

European country. The data includes 1,218,293 nodes and 21,907,608 temporal edges over a 19 day period. We computed the expected frequencies of 2- and 3- node motifs with 3 edges at a time scale of  $\delta = T = 24$  hours with 19 intervals, and  $C_1 = C_2 = 4$ . Figure 6 shows that our model accurately follows the trends in motif counts, particularly the dip in motifs around weekends, but does not fit the actual numbers of motifs. We explain this by the very localized nature of the phonecall network where both the temporal activity as well as community structure of nodes would need to be modeled. We note that our TASBM is easily extendable to that setting as well.

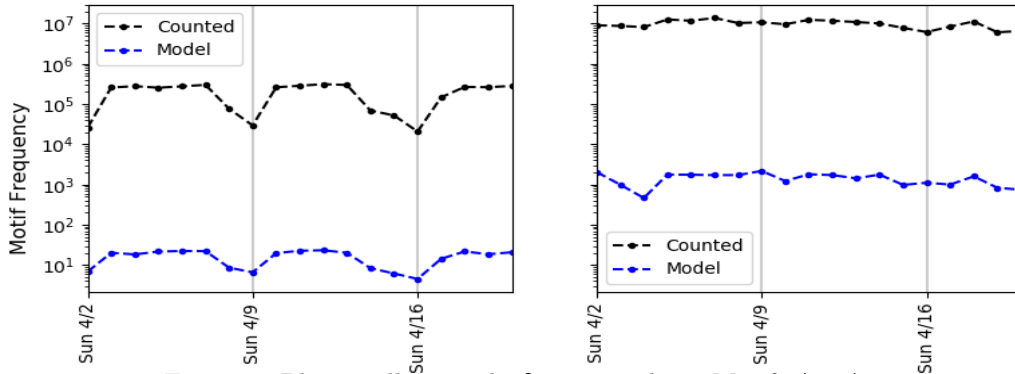


Figure 6: Phone call network,  $\delta = T = 90$  days. Motifs A1, A5.

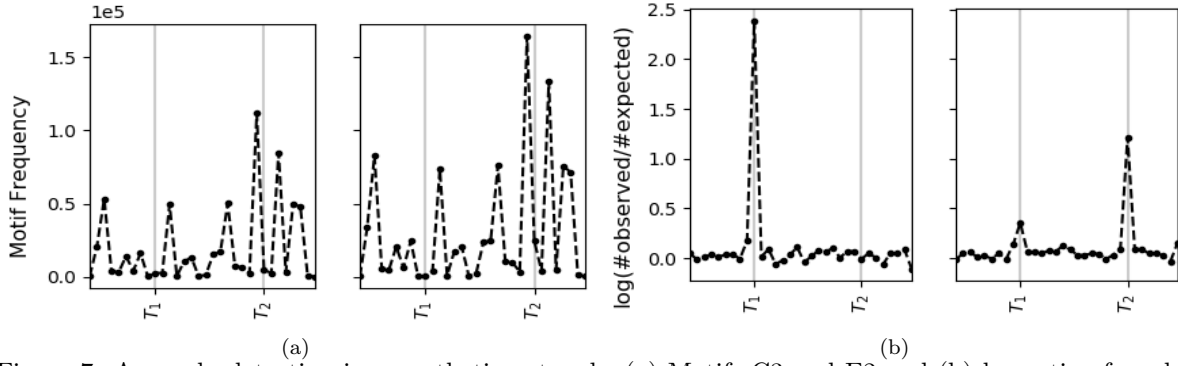


Figure 7: Anomaly detection in a synthetic network. (a) Motifs C3 and E2 and (b) log ratio of model and counting comparison for motifs C3 and E2. Notice the spikes in log ratio where anomalies occur.

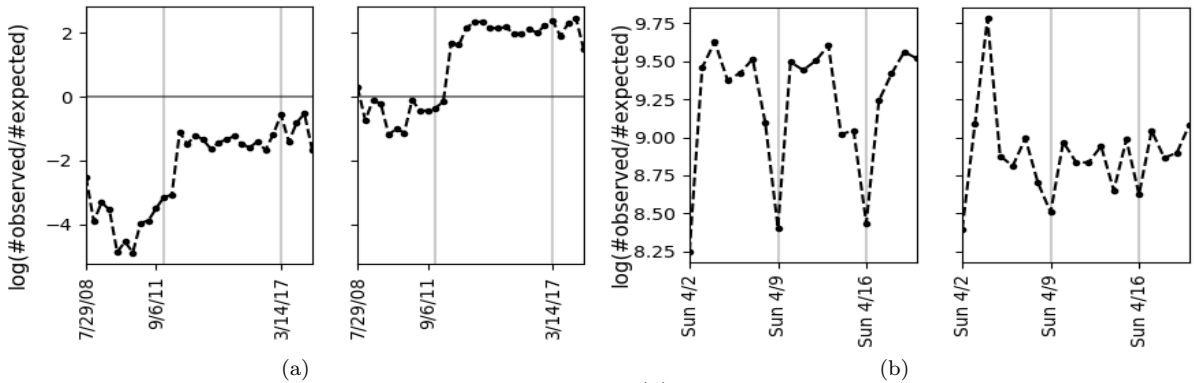


Figure 8: Anomaly detection in real-world networks: (a) financial transaction motifs F1 and A6 and (b) phone call motifs A1 and A5. Notice the spikes in log ratios at the times when anomalies occurred.

## 5.4 Anomaly Detection

**Identifying Synthetic Planted Anomalies.** We next show how our framework can be used to identify motif anomalies. We generate a 100 node network over 32 distinct intervals of 1000 time steps with randomly chosen edge arrival rates. In addition, on the 10-th time interval (labeled  $T_1$  in Figures 7a and 7b) we plant anomalous reciprocated edges and on interval 25 (labeled  $T_2$ ) we plant anomalous repeated edges. We introduce both anomalies by the following process: after an edge is drawn from the Poisson process, we generate a corresponding anomalous edge with probability 0.25, and place it at a random time within the next 10 and 100 steps.

We show that observed motif counts alone are not sufficient to identify planted motif anomalies. C3 has a reciprocated edge and E2 has a repeated edge, so the anomaly at  $T_1$  should impact the number of instances of C3 while the anomaly at  $T_2$  should impact the number of instances of E2. Figure 7a shows the number of instances of motifs C3 and E2 over time, in which neither planted motif is notable. Figure 7b shows the log of the ratio of counted and modeled motif frequencies. Here, we immediately see which motifs are most affected by the anomalies at  $T_1$  and  $T_2$ .

**Real-World Anomaly Detection.** Finally, we examine the log ratio of counted and modeled motif frequencies on real-world datasets to identify where our model most differs from the actual motif instances. Figure 8a shows this ratio for the financial transaction network. While the actual motif counts only go down slightly over time (Figure 4) it is notable that in September of 2011, when a financial crisis hit the country, the number of modeled motifs dropped significantly, so the ratio changed as well. In Figure 8b we see that the model's values for motifs A1 and A5 are more accurate on Sundays, especially A1 (a triangle).

## 6 Discussion

We have developed an analytical model to determine the expected number as well as the variance of motifs in a temporal network. We developed an efficient parameter inference technique as well as provided closed form solutions for the expected motif frequencies in the general case where temporal edges appear with distinct rates between different pairs of nodes, and the arrival rate of temporal edges between every pair of nodes may change over time. We demonstrated the effectiveness of our Temporal Activity State Block Model combined with our analytical model of temporal motifs for modeling temporal networks and detecting anomalies. Applied to a financial transaction network, our framework can successfully localize anomalies caused by a financial crisis. Moreover, we identify trends such as weekends by looking at the significance profile of temporal motifs in a phone call network.

## References

- [1] A. Ahmed and E. P. Xing. Recovering time-varying networks of dependencies in social and biological studies. *PNAS*, 106(29):11878–11883, 2009.
- [2] P. Bajardi, A. Barrat, F. Natale, L. Savini, and V. Colizza. Dynamical patterns of cattle trade movements. *PLoS one*, 6(5):e19869, 2011.
- [3] A. R. Benson, D. F. Gleich, and J. Leskovec. Higher-order organization of complex networks. *Science*, 353(6295):163–166, 2016.
- [4] M. Corneli, P. Latouche, and F. Rossi. Modelling time evolving interactions in networks through a non stationary extension of stochastic block models. In *ASONAM*, pages 1590–1591, 2015.
- [5] A. Decelle, F. Krzakala, C. Moore, and L. Zdeborová. Asymptotic analysis of the stochastic block model for modular networks and its algorithmic applications. *Physical Review E*, 84(6):066106, 2011.
- [6] T. Donker, J. Wallinga, and H. Grundmann. Dispersal of antibiotic-resistant high-risk clones by hospital networks: changing the patient direction can make all the difference. *Journal of Hospital Infection*, 86(1):34–41, 2014.
- [7] S. Gurukar, S. Ranu, and B. Ravindran. Commit: A scalable approach to mining communication motifs from dynamic networks. In *Proceedings of the ACM SIGMOD International Conference on Management of Data*, pages 475–489, 2015.
- [8] Q. Ho, L. Song, and E. Xing. Evolving cluster mixed-membership blockmodel for time-evolving networks. In *AISTATS*, pages 342–350, 2011.
- [9] P. Holme and F. Liljeros. Birth and death of links control disease spreading in empirical contact networks. *Scientific reports*, 4:4999, 2014.
- [10] L. Kovanen, M. Karsai, K. Kaski, J. Kertész, and J. Saramäki. Temporal motifs in time-dependent networks. *Journal of Statistical Mechanics: Theory and Experiment*, 2011(11):P11005, 2011.
- [11] M. Li, V. D. Rao, T. Gernat, and H. Dankowicz. Lifetime-preserving reference models for characterizing spreading dynamics on temporal networks. *Scientific reports*, 8(1):709, 2018.
- [12] P. Liu, A. Benson, and M. Charikar. A sampling framework for counting temporal motifs. *arXiv preprint arXiv:1810.00980*, 2018.
- [13] C. Matias and V. Miele. Statistical clustering of temporal networks through a dynamic stochastic block model. *Journal of the Royal Statistical Society: Series B (Statistical Methodology)*, 79(4):1119–1141, 2017.



- [14] M. E. Newman. The structure and function of complex networks. *SIAM review*, 45(2):167–256, 2003.
- [15] A. Paranjape, A. R. Benson, and J. Leskovec. Motifs in temporal networks. In *WSDM*, pages 601–610. ACM, 2017.
- [16] U. Redmond and P. Cunningham. Temporal subgraph isomorphism. In *ASONAM*, pages 1451–1452. IEEE, 2013.
- [17] T. Squartini, I. Van Lelyveld, and D. Garlaschelli. Early-warning signals of topological collapse in interbank networks. *Scientific reports*, 3:3357, 2013.
- [18] A. H. Westveld, P. D. Hoff, et al. A mixed effects model for longitudinal relational and network data, with applications to international trade and conflict. *The Annals of Applied Statistics*, 5(2A):843–872, 2011.
- [19] K. S. Xu and A. O. Hero. Dynamic stochastic blockmodels: Statistical models for time-evolving networks. In *SBP*, pages 201–210. Springer, 2013.
- [20] T. Yang, Y. Chi, S. Zhu, Y. Gong, and R. Jin. Detecting communities and their evolutions in dynamic social networks—a bayesian approach. *Machine learning*, 82(2):157–189, 2011.
- [21] X. Yu, T. Pei, K. Gai, and L. Guo. Analysis on urban collective call behavior to earthquake. In *HPCC*, pages 1302–1307, 2015.
- [22] Q. Zhao, Y. Tian, Q. He, N. Oliver, R. Jin, and W.-C. Lee. Communication motifs: a tool to characterize social communications. In *CIKM*, pages 1645–1648, 2010.

## A Appendix

### A.1 Additional Figures

Here we provide additional figures explaining our analytical model. Figure 10 gives examples of joint instances of motifs, used in computing variance. Figure 11 shows how multiple distinct motif instances may correspond to the same activity state assignment, a key feature in reducing the complexity of our model.

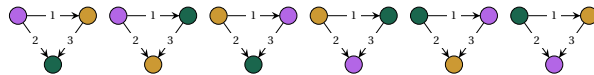


Figure 9:  $3! = 6$  unique bijections between a 3-node 3-edge subgraph and the motif in Figure 1b. Some of these bijections correspond to the same static graph, but the ordering on the temporal motif edges are different.

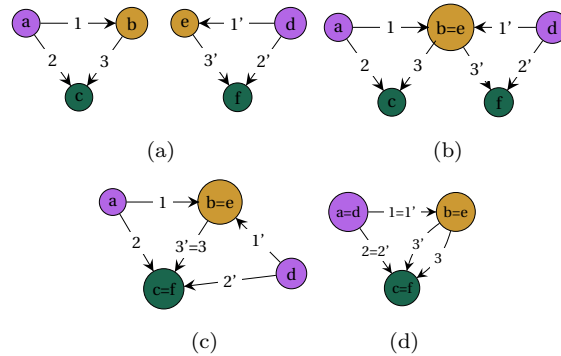


Figure 10: Examples of joint instances of motif  $M$ :  $S_1$  on vertices  $(a, b, c)$  with edges labeled 1, 2, and 3 at times  $t_1 < t_2 < t_3$  and  $S_2$  on vertices  $(d, e, f)$  with edges labeled 1', 2', and 3' at times  $t_{1'} < t_{2'} < t_{3'}$ .

Time Interval	Analytical Model	Random Graph Counting
1e3	6.40	10.2
1e5	6.50	10.6
1e7	6.45	164

Table 2: Average run times in seconds for analytical model and randomized ensemble of 100 graphs. Input to each test is the same set of 36 activity state group sizes with corresponding rates over increasing time intervals.

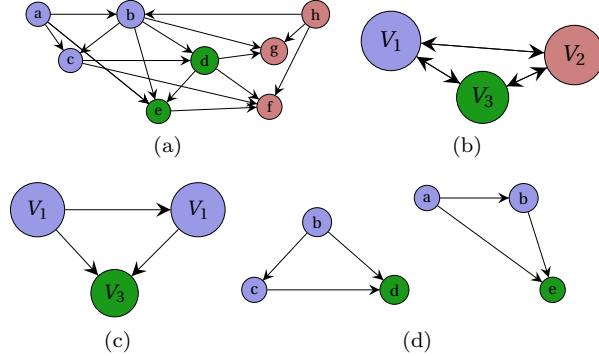


Figure 11: (a) Example graph, (b) assignment of partition  $V = \{V_1, V_2, V_3\}$ , (c) activity state assignment to a motif, and (d) two instances of motifs with the assigned activity states.

## A.2 Implementation Details

Our C++ implementation of the model can be found at:

<https://www.dropbox.com/sh/81tkcf1amemmq2i/AAC2k1vdX2DhsbFQz9LCzovEa?dl=0>

Also included is the set of synthetic graph generators and the setup for comparing our model’s run time to motif counting on randomly generated graphs. We use the implementation of temporal motif counting from [15] included in the Snap library, available at: <http://snap.stanford.edu/snap/index.html>

The European research institute email network dataset is publicly available and can be found at:

<http://snap.stanford.edu/data/email-EuAll.html>

We pre-processed all datasets by sorting by timestamp and relabeling nodes as integers appearing in increasing order; the derived sets from the email dataset can also be found with our code. We also constructed a further processed graph by removing nodes with degree less than 10% the maximum degree, and then selecting the subgraph induced by the remaining nodes forming the largest community.

Table 2 shows the timings results of our model and for counting motifs over randomly generated graphs. The average motif counts in synthetic graphs generated according to the activity state block model will converge to the values generated by our analytical model. For each of the two methods, we measured the run time on average over 100 trials. For the analytical model a trial consists of generated expected motif values from the TASBM state groups and edge arrival rates. State groups and edge arrival rates for all timing experiments were derived from fitting the model on the financial transaction network. There are approximately 13,000 nodes and the number of edges in each experiment ranged from about 200 in the shortest time interval to approximately 1.8 million in the longest. For the random ensemble method, a trial consists of generating a random graph according to the activity state blocks in the TASBM and then counting motif instances. In practice, the random graph counting method would need to run multiple trials and average the resulting motif counts to achieve approximately the same values as the analytical model, so the run time would be even greater than shown here, e.g. 100 times longer to get the average motif counts over an ensemble of 100 random graphs.

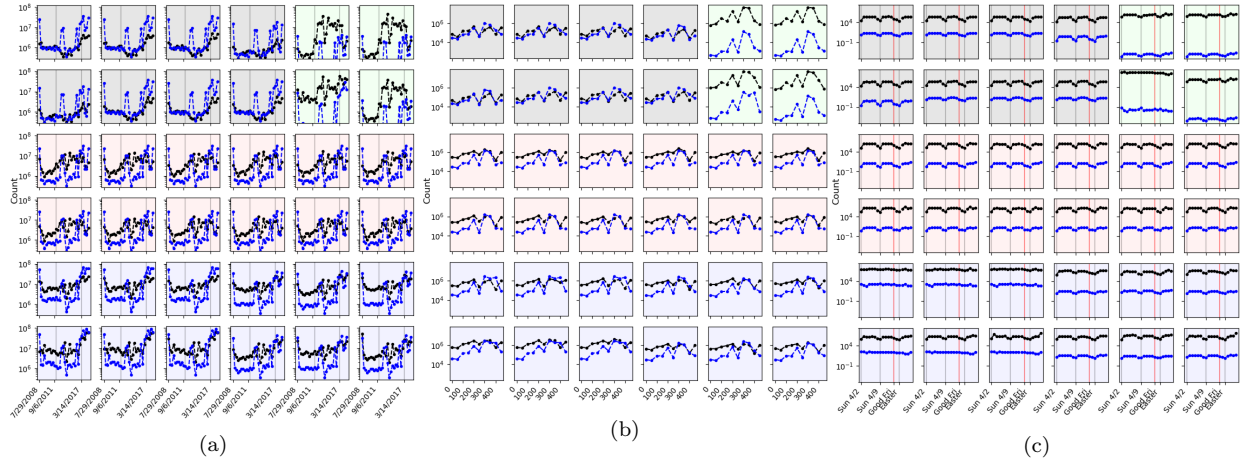


Figure 12: Counted (black) and TASBM (blue) motif results on all 36 motifs: (a) financial transaction network (b) email network and (c) phone call network.

### A.3 Additional Experiments

Here we show the result of our experiments on the full set of 36 motifs. Plots are organized corresponding to Figure 2. Figure 12 includes the experiments shown in Section 5.3 and Figure 13 includes the experiments show in Section 5.4.

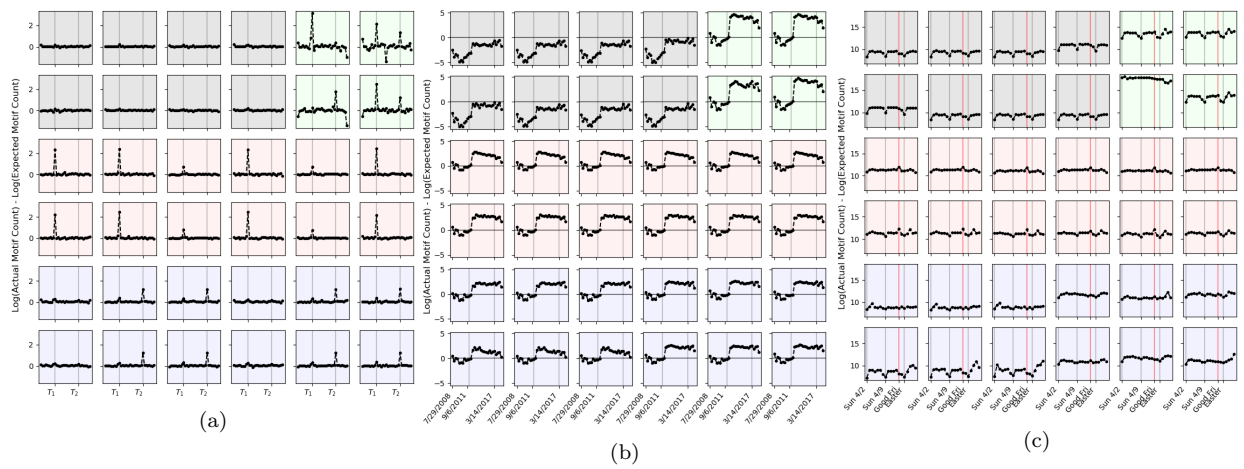


Figure 13: Logarithm of ratio between counted and TASBM motif instances for (a) synthetic network with planted anomalies (b) financial transaction network and (c) phone call network.